





ORIGINAL ARTICLE

The molecular diagnosis of rejection in liver transplant biopsies: First results of the INTERLIVER study

Katelynn Madill-Thomsen¹ | Marwan Abouljoud² | Chandra Bhatti³ | Michał Ciszek⁴ | Magdalena Durlak⁵ | Sandy Feng⁶ | Bartosz Foronczewicz⁴ | Iman Francis² | Michał Grąt⁷ | Krzysztof Jurczyk⁸ | Goran Klintmalm⁹  | Maciej Krasnodębski⁷ | Geoff McCaughan¹⁰ | Rosa Miquel¹¹ | Aldo Montano-Loza¹² | Dilip Moonka² | Krzysztof Mucha⁴ | Marek Myślak¹³ | Leszek Pączek⁴ | Agnieszka Perkowska-Ptasińska⁵ | Grzegorz Piecha¹⁴ | Trevor Reichman³  | Alberto Sanchez-Fueyo¹¹  | Olga Tronina⁵ | Marta Wawrzynowicz-Syczewska⁸ | Andrzej Więcek¹⁴ | Krzysztof Zieniewicz⁷ | Philip F. Halloran^{1,12} 

¹Alberta Transplant Applied Genomics Centre, Edmonton, Alberta, Canada

²Henry Ford Hospital, Detroit, Michigan

³Virginia Commonwealth University, Richmond, Virginia

⁴Department of Immunology, Transplantology and Internal Diseases, Medical University of Warsaw, Warsaw, Poland

⁵Department of Transplant Medicine, Nephrology and Internal Diseases, Medical University of Warsaw, Warsaw, Poland

⁶University of California San Francisco, San Francisco, California

⁷Department of General, Transplant and Liver Surgery, Medical University of Warsaw, Warsaw, Poland

⁸Department of Infectious Diseases, Hepatology and Liver Transplantation, Pomeranian Medical University, Szczecin, Poland

⁹Baylor University Medical Center, Dallas, Texas

¹⁰Centenary Research Institute, Australian

Molecular diagnosis of rejection is emerging in kidney, heart, and lung transplant biopsies and could offer insights for liver transplant biopsies. We measured gene expression by microarrays in 235 liver transplant biopsies from 10 centers. Unsupervised archetypal analysis based on expression of previously annotated rejection-related transcripts identified 4 groups: normal “R1_{normal}” (N = 129), T cell-mediated rejection (TCMR) “R2_{TCMR}” (N = 37), early injury “R3_{injury}” (N = 61), and fibrosis “R4_{late}” (N = 8). Groups differed in median time posttransplant, for example, R3_{injury} 99 days vs R4_{late} 3117 days. R2_{TCMR} biopsies expressed typical TCMR-related transcripts, for example, intense IFNG-induced effects. R3_{injury} displayed increased expression of parenchymal injury transcripts (eg, hypoxia-inducible factor EGLN1). R4_{late} biopsies showed immunoglobulin transcripts and injury-related transcripts. R2_{TCMR} correlated with histologic rejection although with many discrepancies, and R4_{late} with fibrosis. R2_{TCMR}, R3_{injury}, and R4_{late} correlated with liver function abnormalities. Supervised classifiers trained on histologic rejection showed less agreement with histology than unsupervised R2_{TCMR} scores. No confirmed cases of clinical antibody-mediated rejection (ABMR) were present in the population, and strategies that previously revealed ABMR in kidney and heart transplants failed to reveal a liver ABMR phenotype. In conclusion,

Abbreviations: AA, archetypal analysis; ABMR, antibody-mediated rejection; ABMR-RATs, antibody-mediated rejection rejection-associated transcripts; BATs, B cell-associated transcripts; cIRITs, cardiac injury and repair-induced transcripts; DAMPs, damage-associated molecular pattern-associated transcripts; eDSASTs, endothelial donor-specific antibody-selective transcripts; ENDATs, endothelial cell-associated transcripts; FICOLs, fibrillar collagen transcripts; GRITs, gamma-interferon and rejection-associated transcripts; IGTs, immunoglobulin transcripts; IQR, interquartile range; IRITD3, injury and rejection-induced transcripts—intermediate; IRITD5, injury and rejection-induced transcripts—late; IRRATs, injury-repair-associated transcripts; MCATs, mast cell-associated transcripts; MMDx, Molecular Microscope[®] Diagnostic System; PBTs, pathogenesis-based transcripts; PCA, principal component analysis; PCs, principal components; QCATs, quantitative CTL-associated transcripts; RATs, rejection-associated transcripts; Rej-RATs, rejection-associated transcripts; SOC, standard-of-care; TCMR, T cell-mediated rejection; TCMR-RATs, T cell-mediated rejection-associated transcripts.

The MMDx-Liver study group is detailed in Table S1.

[Correction added on April 16, 2020, after first online publication: The author name ‘Chandra Bhatti’ in the author byline has been corrected to Chandra Bhatti.]

© 2020 The American Society of Transplantation and the American Society of Transplant Surgeons

National Liver Transplant Unit, Royal Prince Alfred Hospital, The University of Sydney, Sydney, NSW, Australia

¹¹King's College London, London, UK

¹²University of Alberta, Edmonton, Alberta, Canada

¹³Department of Clinical Interventions, Department of Nephrology and Kidney, Transplantation, SPWSZ Hospital, Pomeranian Medical University, Szczecin, Poland

¹⁴Department of Nephrology, Transplantation and Internal Medicine, Medical University of Silesia, Katowice, Poland

Correspondence

Philip F. Halloran

Email: phallora@ualberta.ca

Funding information

Genome Canada; Canada Foundation for Innovation; University of Alberta Hospital Foundation; Alberta Ministry of Advanced Education and Technology; Mendez National Institute of Transplantation Foundation; Industrial Research Assistance Program; Roche Organ Transplant Research Foundation; Thermo Fisher

molecular analysis of liver transplant biopsies detects rejection, has the potential to resolve ambiguities, and could assist with immunosuppressive management.

KEYWORDS

basic (laboratory) research/science, biopsy, liver transplantation/hepatology, microarray/gene array, molecular biology: mRNA/mRNA expression, rejection

1 | INTRODUCTION

Diagnosis of rejection in liver transplantation remains an important issue in clinical management.¹⁻⁴ The current standard-of-care (SOC) for liver biopsy diagnoses is histology, generally following Banff guidelines.⁵ Histology is based on pattern recognition by experts, and assessments differ between observers.⁶⁻¹¹ Reported kappa values for pathology related to T cell-mediated rejection (TCMR) are low to moderate (0.15-0.62¹²) especially when comorbidities are present,⁷ leaving an unmet need for improvement in precision. Moreover, the diagnosis and prevalence of antibody-mediated rejection (ABMR) in liver transplants remain controversial.^{5,13-15} Liver transplants present unique challenges because of their tolerogenic properties, inviting clinicians to consider reducing immunosuppression.¹⁶⁻²⁰ However, this practice requires a precise and accurate system for diagnosing rejection.²¹⁻²⁵ Liver function test abnormalities are associated with rejection but cannot distinguish TCMR from other diseases such as steatohepatitis.^{26,27}

Molecular measurement of gene expression using microarrays coupled with machine learning has the potential to improve the assessment of transplant biopsies by overcoming the limitations of conventional diagnostics.²⁸ We previously developed the Molecular Microscope[®] Diagnostic System (MMDx) for kidney,²⁹⁻³² heart,^{33,34} and lung transplants.³⁵⁻³⁷ A number of factors argue that MMDx testing is more accurate than histology²⁹: for example, use of continuous quantitative measurements,²⁹ low sampling error,³⁰ high reproducibility,³⁰ and lack of requirements for specific tissue elements such as glomeruli, cortex, or portal triads. MMDx predicts outcomes better

than histologic assessments.³⁸⁻⁴³ Many major rejection and injury features initially described in kidney transplants^{31,44,45} are shared with heart^{33,46-48} and lung transplants,^{35,49} indicating that rejection changes are not organ specific and are likely shared by liver transplants. Existing studies have established the potential utility of molecular assessment of liver biopsies.^{1,24-25,50-56}

Given the advantages of molecular diagnostics discussed previously, the present study aimed to develop an MMDx system for diagnosing rejection in liver transplant biopsies using microarray measurements of gene expression plus machine learning to interpret the output in terms of injury and rejection. We used unsupervised analysis based on expression of rejection-associated transcripts (RATs) derived in kidney transplants⁵⁷ and validated in heart and lung and evaluated the potential for supervised analyses based on histology features. This alternative approach was compared to the local SOC from the participating centers, to assess the potential clinical impact that MMDx testing presents in liver transplantation.

2 | MATERIALS AND METHODS

2.1 | Population and demographics

We studied 235 biopsies prospectively collected from 217 liver transplant patients in 10 international centers during the INTERLIVER study (ClinicalTrials.gov NCT03193151, Table S1). All biopsies were stabilized in RNAlater[™] and shipped at ambient temperature to

Alberta Transplant Applied Genomics Centre for analysis per established protocols.³¹ Clinical data were reported by the participating centers per SOC. Because donor-specific antibody (DSA) testing is not SOC at most centers, most biopsies were not accompanied by DSA assessment. Histologic classifications were assigned locally at each of the centers nominally using Banff criteria (Table S1).

2.2 | Microarray analysis

Total RNA was extracted and labeled with the Affymetrix-Thermo Fisher IVT 3' Plus kit and hybridized to PrimeView GeneChip microarrays (Thermo Fisher Scientific, Santa Clara, CA) per established protocols.³¹ The .CEL files are available at Gene Expression Omnibus (GEO) (GSE145780).

2.3 | Rejection-associated transcripts

Rejection-associated transcripts (RATs) were derived in kidney transplants and validated in heart^{34,58,59} and lung transbronchial and mucosal biopsies.^{36,37} The RATs are the union of the top 200 Affymetrix probe sets associated with 3 class comparisons based on histology labels: all-rejection (ABMR, TCMR, or Mixed) vs everything else (EE), ABMR vs EE, and TCMR vs EE⁶⁰ (all-rejection and TCMR transcripts were also identified in mouse TCMR models⁴⁴). After removing duplicates, 453 RAT transcripts remained. Some transcripts were identified by more than 1 algorithm, producing 6 classes of RATs as shown in Figure 1A: ABMR-selective (blue), TCMR-selective (red), all-rejection (green), ABMR/all-rejection (cyan), TCMR/all-rejection (orange), and ABMR/TCMR/all-rejection (black).

Interquartile range (IQR) filtering was performed with a cutoff of 0.35 to remove low variance transcripts, producing a final set of 417 transcripts.

2.4 | Pathogenesis-based transcript sets

Pathogenesis-based transcript sets (PBTs) associated with biological mechanisms in rejection and injury were previously annotated in human cell lines, mouse experimental models, and human transplant biopsies⁶¹ (<https://www.ualberta.ca/medicine/institutes-centres-groups/atagc/research/gene-lists>). PBTs have been extensively used in liver transplant studies.^{62,63} PBT values represent the mean fold change in expression compared to a control group. Biopsies assigned to the R1 group by highest archetype score were used as the control. For these analyses, we selected the following PBTs: ABMR-selective (ABMR-RATs),⁵⁸ B cell-associated (BATs),⁶⁴ cardiac injury and repair-induced (cIRITs),⁶⁵ damage-associated molecular pattern-associated (DAMPs),⁶⁶ endothelial donor-specific antibody-selective (eDSASTs),⁶⁷ endothelial cell-associated (ENDATs),⁶⁸ gamma-interferon and rejection-associated (GRITs),⁶⁹ immunoglobulin (IGTs),⁶⁴ injury and rejection-induced at day 3 (IRITD3)

and day 5 (IRITD5),⁷⁰ injury-repair-associated (IRRATs),⁷¹ mast cell-associated (MCATs),⁷² quantitative CTL-associated (QCATs),⁷³ ABMR-selective plus TCMR-selective plus all-rejection-associated (RATs),⁵⁸ all-rejection-associated (Rej-RATs),⁵⁸ TCMR-selective (TCMR-RATs),⁵⁸ and fibrillar collagens (FICOLs).

2.5 | Principal component analysis

Principal component analysis (PCA) was used to visualize the biopsies based on their expression of the 417 RAT transcripts. All PC-based analyses were done in base R⁷⁴ using the "FactoMineR" package.⁷⁵ PCs for Figure 1B-G were established based on the RAT expression within each organ (kidney N = 1526, heart N = 1320, and liver N = 235).

2.6 | Archetypal analysis (AA)

AA is a clustering method that identifies a limited number (*n*) of theoretical idealized extreme phenotypes called archetypes (A1, A2, A3, and A4) and assigns each biopsy *n* scores to describe its proximity to each archetype. By convention, AA also assigns biopsies to clusters (R1, R2, R3, and R4) based on their highest archetype score, providing a completely objective method of classifying the biopsies into groups for analysis. The scree plot "elbow method" combined with the knowledge of clinical liver phenotypes and previous AA experience^{33,36,76} determined the appropriate number of major biopsy groups. AA was performed using the "archetypes" package for R version 1.1.463.⁷⁷

2.7 | Moving averages

Moving average plots were generated in R version 3.5.1 using the "zoo" package.⁷⁸ A window size of 75 was used for each graph.

2.8 | Supervised analysis

SOC rejection in these centers was usually reported as lesion grades plus text commentary rather than discrete classes (rejection vs no rejection). Thus for comparison with MMDx, biopsies were classified as histologic rejection (TCMR) vs no rejection (NR), on the basis of their summed portal, bile duct, and venous inflammation grades.^{5,79} Biopsies were considered positive for histologic rejection if the sum of these grades was >0 (alternate analyses used >1 or >2). Biopsies with inadequate information were excluded (N = 15).

Relationships with SOC histologic features were considered significant if their Spearman correlation coefficient values were above the arbitrarily assigned cutoff of 0.2. All correlations above this cutoff had significant *P* values (*P* < .001).

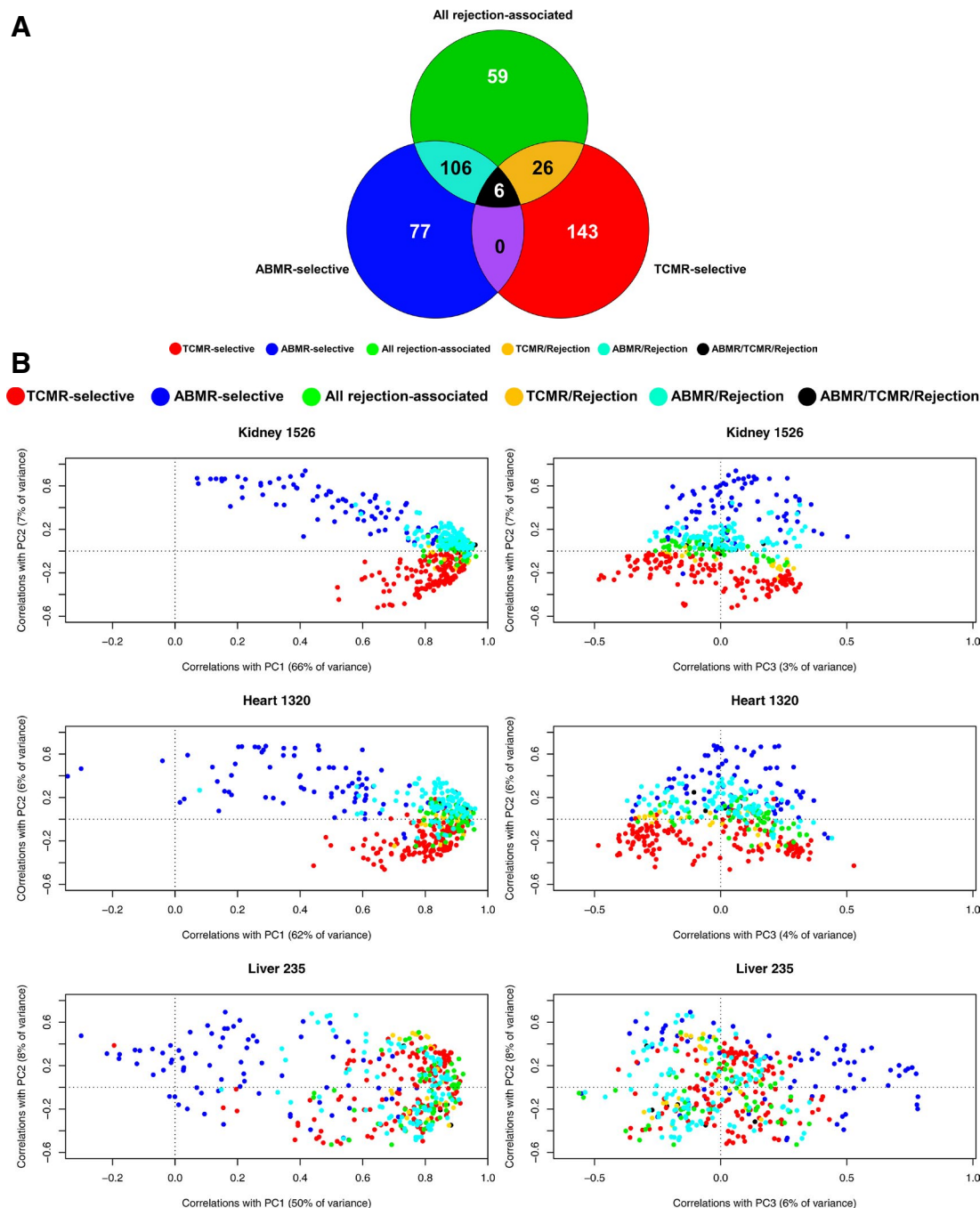


FIGURE 1 (A) Venn diagram of the rejection-associated transcripts (RATs). RAT transcripts were divided into 6 groups: all-rejection RATs (green, "Rejection-RATs"), T cell-mediated rejection (TCMR)-RATs (red), and antibody-mediated rejection (ABMR)-RATs (blue), as well as the overlap groups TCMR/rejection (orange), ABMR/rejection (cyan), and ABMR/TCMR/rejection (black) that were identified by more than one algorithm. The Venn diagram shows the RATs as they are assigned to ABMR, TCMR, and all-rejection ("Rejection") in kidney transplant biopsies ($N = 1679$), and the corresponding overlaps (transcripts common to multiple categories). Note that the relatively low overlap between All rejection (green) and TCMR (red) and between All rejection and ABMR (blue) is because there are differences in highest 200 ranks. There is more overlap when lower ranks are included. (B-G) Plots showing the correlation of each of the rejection-associated transcripts (RATs) with the principal components (PCs) in kidneys, hearts, and livers. Each dot represents a single RAT transcript. The position of the dot is determined by its Pearson correlation with PC1, PC2, and PC3, derived in biopsy sets from each organ (see Materials and Methods). The RATs are shown in kidneys (Panel B showing PC1 vs PC2 and Panel C showing PC3 vs PC2), and in hearts (Panel D showing PC1 vs PC2 and Panel E showing PC3 vs PC2) for comparison. The distribution of RATs in liver biopsies is shown in Panel F (PC1 vs PC2) and Panel G (PC3 vs PC2).

2.9 | Statistical analysis

All statistics were performed in base R version 3.5.1.⁷⁴ Areas under the curve (AUCs) and comparisons were done using “pROC.”⁸⁰ All correlations were calculated as Spearman correlations (with the exception of Pearson correlations in Figure 1B-G).

2.10 | MMDx diagnosis assignment

As a first-generation biopsy report interpretation, guidelines for diagnosing TCMR included the AA grouping, the position of the biopsy in the reference set on page 1 and the PBT scores on page 2: TCMR = $PC1 > 0 + PC3 < 0$ + abnormal TCMR-related PBTs (all) + abnormal Rejection-RATs and GRITs + R2 assignment by archetypes (or very high R2 score). The term “abnormal” describes PBT scores for a biopsy that exceed the 80th percentile of biopsies with the $R1_{normal}$ score ≥ 0.7 (relatively normal biopsies).

3 | RESULTS

3.1 | Study population and demographics

We prospectively analyzed 235 biopsies from 217 patients (Table S1), with 170 biopsies (72%) taken for indications (Table 1). Median time posttransplant (TxBx) was 962 days (range 0-11,676 days). DSA testing per center practice was performed in only 17 biopsies (10

positive, Table S2). RNA extracted from these biopsies (average length 4.5 mm, range 0.5-14 mm of 16- or 18-gauge core) was high yield (average 9.91 μ g RNA, range 0.28-73 μ g) and high quality (average RNA integrity number 8.2). The technical replication of results in a single RNA sample (extracted from kidney transplant biopsies) processed independently by 2 technicians using 2 microarrays showed 99% replication of PC1, PC2, PC3, and the archetype scores from the molecular report.^{30,32} The agreement between 2 pieces from 1 liver biopsy processed separately was tested in 10 cases and showed very high agreement (data not shown).

3.2 | Principal component analysis

We used PCA to plot the population in terms of its expression of RAT genes. PC1, 2, and 3 comprised 66%, 7%, and 3% of the variation, respectively.

Figure 1B-G shows the correlation of each RAT transcript with PC1, PC2, and PC3 for the liver biopsies, compared to published analyses for kidney and heart biopsies,⁵⁸ adapted to permit comparison with liver biopsies. The location of the transcripts in this factor map was used to establish an appropriate interpretation of the actual biopsies in PCA: for example, if TCMR-RATs are located toward the right side of the plot, biopsies located to the right will likely have molecular TCMR.

In each organ population, Rejection-RATs and TCMR-RATs were strongly associated with PC1. In kidneys (Figure 1B,C) and hearts (Figure 1D,E), the ABMR-RATs (blue) and ABMR-all-rejection RATs

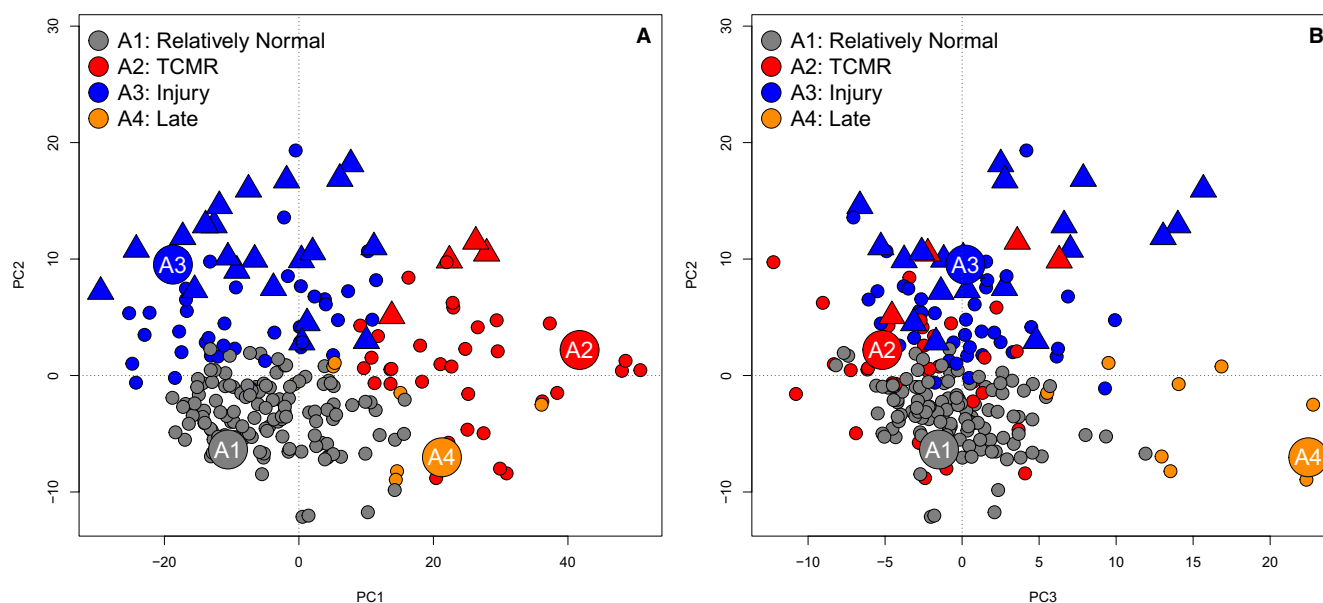


FIGURE 2 Unsupervised archetypal rejection-based analysis of 235 (218 patients) liver transplant biopsies. Liver biopsies were separated by their expression of rejection-associated transcripts (RATs) in PCA. Archetypal analysis identified four major phenotypes, or “archetypes”: A1, A2, A3, and A4. Each biopsy was given four archetype scores describing their similarity to each archetype. Biopsies are grouped by their highest archetype score into clusters: R1 (N=129), R2 (N=37), R3 (N=61), and R4 (N=8). Panel B plots principal component 2 vs. principal component 1, and panel C plots principal component 2 vs. principal component 3. Triangles represent biopsies taken in the first two weeks post-transplant. Groups were named based on characterization by gene expression (see Results).

TABLE 1 INTERLIVER patient and biopsy characteristics

Patient characteristics		Patients N = 217	
Recipient sex (% total)			
Male		107 (49%)	
Female		110 (51%)	
Recipient age at transplant (median, range)		50 (2-71)	
Primary disease (% total) ^a			
Alcoholic liver disease		31 (14%)	
Autoimmune hepatitis		20 (9%)	
Hepatitis B		13 (6%)	
Hepatitis C		35 (16%)	
Hepatocellular carcinoma		21 (10%)	
Nonalcoholic steatohepatitis		15 (7%)	
Primary biliary cholangitis		15 (7%)	
Primary sclerosing cholangitis		24 (11%)	
Other		30 (14%)	
Missing		39 (18%)	
Biopsy characteristics		Biopsies N = 235	
Days (median, range) from transplant to biopsy (TxBx)		967 (0-11 676)	
Immunosuppression at biopsy (% total)			
Corticosteroids		1 (<1%)	
Cyclosporine		5 (2%)	
Tacrolimus		108 (46%)	
Missing		171 (73%)	
Indication for biopsy (% total)			
Indication: clinician concerned about graft function		173 (74%)	
Follow-up from previous biopsy		2 (1%)	
Protocol/surveillance		36 (15%)	
Missing		24 (10%)	
Number of biopsies with histologic acute rejection lesions		Present	Absent
Portal inflammation >0		149	73
Bile duct inflammation >0		75	145
Venous inflammation >0		59	161
Sum of lesion scores >0 ^b		162	58
Sum of lesion scores >1 ^b		95	125
Sum of lesion scores >2 ^b		57	163
		NA	15

Note: No biopsies were clearly marked as "ABMR" (antibody-mediated rejection) by the participating centers in this population.

^aSome patients fell under multiple categories.

^bHistologic rejection >x categories were calculated as the sum of their histology grades for portal inflammation, bile duct inflammation, and venous inflammation. Samples with summed histology grade <x were noted as "absent." Biopsies without sufficient information were marked not available (NA).

(cyan) vertically separated from the TCMR-RATs (red) in PC2, indicating distinct ABMR and TCMR rejection states. ABMR/all-rejection RATs (cyan) were particularly instructive because they are strongly associated with ABMR and separate from TCMR-RATs (red) in kidney and heart.

There was no ABMR-TCMR separation of the RATs in liver biopsies (Figure 1F,G); this finding is particularly clear in PC2 vs PC3 (Figure 1G).

RATs not trained in hearts still separated TCMR from ABMR in PC2 in the heart population; thus the lack of separation between ABMR-RATs and TCMR-RATs in liver biopsies was particularly instructive. Assuming that liver ABMR is molecularly similar to heart and kidney ABMR, this finding argues against any sizable ABMR population in this liver biopsy cohort (see Discussion).

3.3 | RAT-based archetypal analysis

We used AA based on RAT expression to visualize biopsy groups.⁷⁶ Supplementary Figure 1 is a scree plot showing the residual sum of squares (y-axis) vs the potential number of archetypes in a model (x-axis). Combined with our expectations based on AA in kidney, heart, and lung, we selected 4 archetypes (highlighted in red): no rejection or injury, rejection (specifically TCMR), early mild injury from donation-implantation, and late changes potentially representing atrophy fibrosis. Because injury activates innate immunity, which shares mechanisms with adaptive immunity, RAT expression is expected to identify some injured biopsies without rejection.

AA assigned 4 archetype scores to each biopsy reflecting its proximity to each archetype. Each biopsy was assigned to an archetype group based on its highest score: R1, N = 129, R2, N = 37, R3, N = 61, and R4, N = 8.

The 4 archetypes and groups of biopsies were distributed in PCA, colored according to their assigned archetype group: PC2 vs PC1 (Figure 2A) and PC2 vs PC3 (Figure 2B). Early biopsies taken within 2 weeks of transplant (triangle symbols) were exclusively in the upper regions of PC2. PC1 separated R2 from R1. PC2 separated R3 biopsies, many of which were early posttransplant. PC3 separated R4 from everything else.

3.4 | Characterizing the groups

In Table 2, the median TxBx of each RAT-based group differed between archetype groups: the earliest in R3 (99 days), and R2 (214 days). R1 was much later at 2534 days and R4 at 3117 days.

R1 biopsies lacked expression of transcripts associated with rejection and injury. R2 biopsies had the highest expression of TCMR-selective (TCMR-RATs), effector T cell (QCATs), and rejection-related PBTs (IFNG-induced GRITs and all-rejection-RATs), and increased expression of injury-related PBTs, particularly DAMPs.

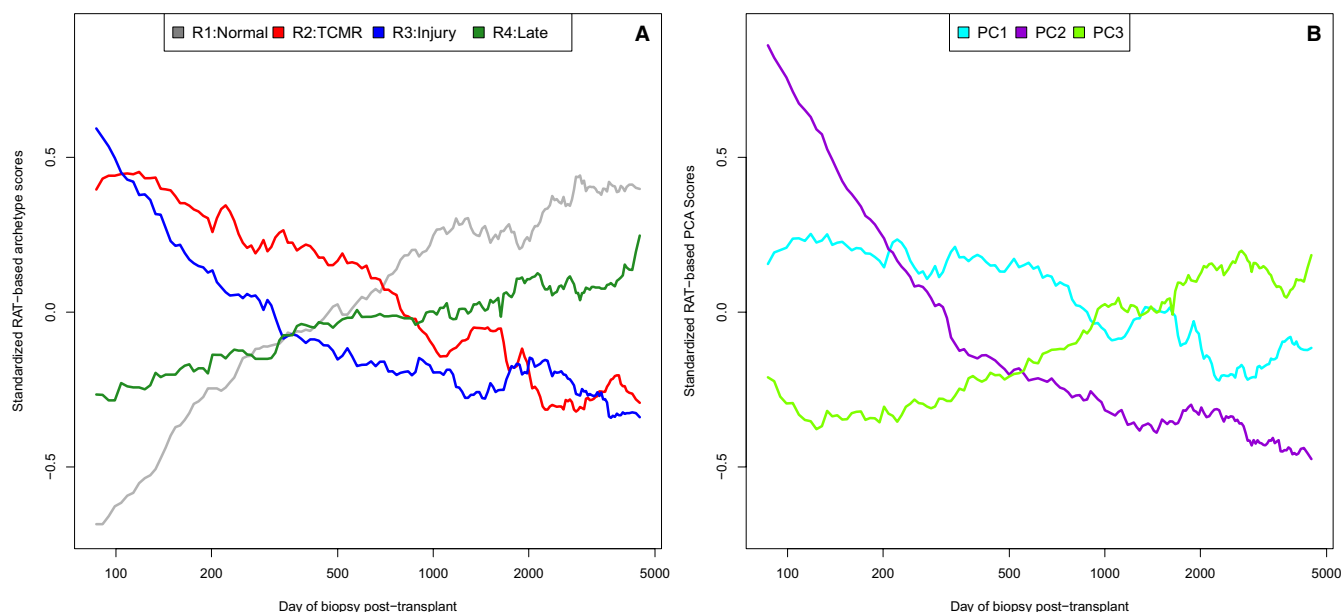


FIGURE 3 Moving average of Rejection (RAT4AA) archetypes (A) and PCA scores (B). Left-aligned 75-sample (Panel A) and 75-sample (Panel B) moving averages were calculated on all 235 liver biopsies ordered by time of biopsy post-transplant. The x-axis tracks the number of days elapsed between transplant and time of biopsy on a logarithmic scale. Scores were normalized in the full set of 235 biopsies. Scores were scaled prior to plotting

R3 biopsies had increased expression of the injury-induced PBTs compared to R1 (eg, IRRATs), with no expression of rejection-related PBTs. R4 biopsies had increased injury-related, moderate elevation of rejection-related, and high expression of endothelium-related and atrophy-fibrosis-related PBTs (IGTs, BATs, and MCATs). Note that the IGTs, BATs, and MCATs have previously been associated with a fibrotic phenotype in liver transplants.⁵⁴

Based on these characteristics, we named the archetypal groups “R1_{normal},” “R2_{TCMR},” “R3_{injury},” and “R4_{late}.”

3.5 | Characterizing the PCs

PC1 correlated with rejection (eg, TCMR-RATs, QCATs, GRITs) and parenchymal injury (eg, DAMPs). PC2 correlated with early TxBx, mild IFNG effects, and mild to moderate elevation of injury parameters (eg, IRITs). PC3 correlated with endothelial-related and late injury-related PBTs (eg, IGTs, BATs, MCATs), moderate elevation of many injury-related PBTs (eg, IRRATs) but without rejection-related PBTs (eg, TCMR-RATs) (Table 3).

3.6 | Transcripts correlated with each RAT archetype score

The top 10 transcripts correlated with each archetype score are summarized in Table 4. We were primarily interested in transcripts lower in R1 and increased in R2-R4 compared to the other groups. The top 30 unique transcripts by Spearman correlation coefficient in R1-R4 are compiled in Tables S3-S6.

The R1_{normal} score was associated with low expression of transcripts previously annotated for associations with transplant injury or rejection (eg, *TRIP1*, *MIR21*, and *IFNGR1*). Top transcripts correlated with the R2_{TCMR} score were typical of TCMR, that is, mainly all-rejection- and TCMR-associated s (eg, *STAT1*, *CXCL11*, and *GBP5*), and all were IFNG inducible, a hallmark of transplant rejection. Top transcripts correlated with the R3_{injury} score reflected injury, including hypoxia-inducible factor *EGLN1*, and many were previously annotated as increased in recent injury models (eg, *PVR*, *PTPN11*, and *SERPINA3*). Top transcripts correlated with the R4_{late} score were previously annotated in injury models (eg, *JAM2*).

3.7 | Time course of molecular scores

We explored the relationship of molecular scores with TxBx using moving average plots (Figure 3). Average standardized R3_{injury} and R2_{TCMR} scores were highest in early biopsies and fell steadily to low levels by 2000 days. Average standardized R1_{normal} scores were initially low but rose steadily to be the dominant score in biopsies after 1000 days. Thus later biopsies frequently had a relatively normal phenotype as they recovered from early donation-implantation injury and as TCMR became less common. High R4_{late} scores became more common in later years posttransplant (Figure 3A).

Similar to the R2_{TCMR} score, PC1 declined slowly over time, likely related to the resolution of early injury and the decline in TCMR. PC2, which is associated with recent injury such as that occurring in donation-implantation, declined sharply over time like the R3_{injury} score. PC3, reflecting late injury, increased steadily like the R4_{late} score (Figure 3B).

3.8 | Correlations with histology

We studied the correlations between the rejection archetype scores, PCA, and the recorded histologic features (Table 5).

PC1 and R2_{TCMR} scores correlated with TCMR-related lesions (portal/bile duct inflammation), and histologic diagnosis of CMV hepatitis. PC2 and R3_{injury} scores, which are features of early biopsies, negatively correlated with fibrosis and positively correlated with recurrent HCV. The PC3 and R4_{late} scores, features of late biopsies, positively correlated with fibrosis.

3.9 | Liver function tests in archetype groups

In Table 6, the R1_{normal} group had the highest albumin values and the lowest bilirubin, aspartate transaminase (AST), alanine transaminase (ALT), and alkaline phosphatase (ALP). The R2_{TCMR} and R3_{injury} groups both had abnormal mean values: R2_{TCMR} had the highest ALP, and R3_{injury} had highest bilirubin and AST. The

R4_{late} group had the lowest albumin, highest bilirubin, and highest ALP.

3.10 | Molecular associations with histologic rejection

Given the associations of the R2_{TCMR} group with histologic rejection features, we performed *t* tests comparing gene expression in biopsies with and without histologic rejection as defined by the >0 threshold. The top 30 differentially expressed genes are shown in Table S7 (adjusted *P* value range .004-.001). Transcripts associated with the R2_{TCMR} score had much smaller *P* values (Table S4, $P = 1.7 \times 10^{-84}$ to 1.2×10^{-56}).

We developed a supervised classifier based on histology rejection lesions >0. The AUC for the molecular rejection scores derived through 10-fold cross-validation for predicting histologic rejection was only 0.57, lower than that for the unsupervised R2_{TCMR} archetype score (0.70, AUCs significantly different, $P = .002$).

TABLE 2 Mean pathogenesis-based transcript (PBT) set scores in biopsies grouped according to their highest Rejection (RAT4AA) archetype score

	R1 _{normal} (n = 129)	R2 _{TCMR} (n = 37)	R3 _{injury} (n = 61)	R4 _{late} (n = 8)
Median time of biopsy posttransplant (in d)	2534	214	99	3117
	Mean PBT score in each archetype group ± SD ^a			
PBT	R1 _{normal}	R2 _{TCMR}	R3 _{injury}	R4 _{late}
TCMR-related transcripts				
TCMR-RAT—TCMR-associated RATs	1 ± 1.25	2.20 ± 1.33	0.99 ± 1.31	1.69 ± 1.33
QCAT—cytotoxic T cell-associated transcripts	1 ± 1.29	2.17 ± 1.39	0.89 ± 1.36	1.78 ± 1.25
Rejection-related				
GRIT—interferon gamma-inducible transcripts	1 ± 1.19	1.84 ± 1.23	1.12 ± 1.33	1.39 ± 1.21
Rejection-RATs—rejection-associated RATs	1 ± 1.26	2.12 ± 1.28	0.95 ± 1.37	1.38 ± 1.33
Endothelium-related transcripts				
eDSAST—endothelium-expressed DSA-selective transcripts	1 ± 1.34	0.84 ± 1.26	0.92 ± 1.56	3.28 ± 1.90
ENDAT—endothelial cell-associated transcripts	1 ± 1.17	1.17 ± 1.22	1.09 ± 1.26	2.13 ± 1.29
Late injury-related transcripts (atrophy-fibrosis)				
IGT—immunoglobulin transcripts	1 ± 1.97	1.38 ± 2.56	0.71 ± 2.01	4.05 ± 2.78
BAT—B cell-associated transcripts	1 ± 1.20	1.32 ± 1.29	0.97 ± 1.22	2.00 ± 1.25
MCAT—mast cell-associated transcripts	1 ± 1.42	0.78 ± 1.36	0.80 ± 1.50	3.12 ± 1.96
Recent injury-related transcripts				
FICOL—fibrillar collagen-associated transcripts	1 ± 1.43	1.49 ± 1.61	1.32 ± 1.69	4.61 ± 1.98
DAMP—damage-associated molecular pattern transcripts	1 ± 1.35	1.48 ± 1.71	1.44 ± 1.94	1.44 ± 2.00
IRRAT—injury/repair-associated transcripts (human kidney)	1 ± 1.34	1.48 ± 1.43	1.33 ± 1.66	2.64 ± 1.64
IRITD3—tissue injury and repair-associated transcripts	1 ± 1.15	1.27 ± 1.18	1.27 ± 1.26	1.88 ± 1.30
IRITD5—tissue injury and repair-associated transcripts	1 ± 1.18	1.42 ± 1.24	1.19 ± 1.26	2.19 ± 1.30
cIRIT—cardiac injury and repair-induced transcripts	1 ± 1.12	1.39 ± 1.17	1.24 ± 1.19	1.52 ± 1.22

Abbreviations: DSA, donor-specific antibodies; TCMR, T cell-mediated rejection.

^aScore represents the mean fold change in PBT expression between biopsies in each archetype group and the R1 biopsies as a control. Biopsies were grouped according to their highest of the 4 archetype scores. The highest score in each row is bolded.

3.11 | Diagnostic interpretation

MMDx diagnoses were assigned by 1 expert (PFH) using a first-generation MMDx-Liver report (Figure 4). The relationship between the molecular scores and histologic rejection is analyzed in Table 7. Use of the >2, >1, or >0 cutoff increased sensitivity but decreased specificity, for example, increased the MMDx no rejection called histologic no rejection from 33% to 80%, but also decreased the

TABLE 3 Correlations between pathogenesis-based transcript (PBT) set scores and Rejection (RAT4AA) PCA scores

PBT	Spearman correlation		
	PC1	PC2	PC3
Correlations with time posttransplant (TxBx)	-0.08	-0.58	0.13
TCMR-related transcripts			
TCMR-RAT–TCMR-associated RATs	0.98	0.07	-0.01
QCAT–cytotoxic T cell-associated transcripts	0.94	-0.09	0.03
Rejection-related			
GRIT–interferon gamma-inducible transcripts	0.91	0.30	-0.02
Rejection-RATs–rejection-associated RATs	0.99	0.05	-0.05
Endothelium-related transcripts			
eDSAST–endothelium-expressed DSA-selective transcripts	0.03	-0.29	0.69
ENDAT–endothelial cell-associated transcripts	0.47	0.06	0.70
Late injury-related transcripts (atrophy-fibrosis)			
IGT–immunoglobulin transcripts	0.44	-0.27	0.36
BAT–B cell-associated transcripts	0.74	-0.09	0.44
MCAT–mast cell-associated transcripts	0.06	-0.47	0.50
Recent injury-related transcripts			
FICOL–fibrillar collagen-associated transcripts	0.42	0.20	0.59
DAMP–damage-associated molecular pattern transcripts	0.33	0.19	0.26
IRRAT–injury/repair-associated transcripts (human kidney)	0.49	0.19	0.53
IRITD3–tissue injury and repair-associated transcripts	0.48	0.48	0.50
IRITD5–tissue injury and repair-associated transcripts	0.65	0.33	0.48
cRIT–cardiac injury and repair-induced transcripts	0.63	0.53	0.28

Note: PBT scores represent the mean fold change in PBT expression between biopsies in each archetype group and the R1 biopsies as a control. Biopsies were grouped according to their highest of the 4 archetype scores. The highest positive score in each row is bolded. Abbreviations: DSA, donor-specific antibodies; TCMR, T cell-mediated rejection.

MMDx rejection called histologic rejection from 89% to 76% and did not significantly change the balanced accuracy (0.60, 0.63, and 0.62, respectively). It was noted that this balanced accuracy was comparable to that seen in previous analyses in heart, and was expected given the known noise in the SOC assessments used for training.

4 | DISCUSSION

This analysis aimed to develop a first-generation MMDx system for liver transplant rejection using RAT expression, unsupervised PCA, and AA and examine its relationship to SOC histology assessments in the center. Small pieces of liver transplant biopsy cores placed in RNAlater™ gave excellent yields of high-quality RNA. In RAT-based PCA, PC1 was highly associated with TCMR-like transcripts, and PC2 correlated with early parenchymal injury. AA identified 4 archetype groups: R1_{normal}, R2_{TCMR}, R3_{injury}, and R4_{late}, each with distinctive top transcripts, PBT associations, time courses, and histology associations. No distinct molecular ABMR group was detected in this unselected biopsy population using strategies that detected ABMR in kidney and heart transplants. Liver function biochemistry was most normal in the R1_{normal} biopsies and comparatively abnormal in other groups. High R3_{injury} and R2_{TCMR} scores were common early and became infrequent at later times, while R4_{late} scores progressively increased with time and correlated with transcripts associated with atrophy-fibrosis. R2_{TCMR} correlated with typical TCMR-like histology changes, and top transcripts reflected IFNG effects, for example, such as TAP1, CXCL9, and CXCL11, hallmarks of TCMR in kidney, heart, and lung transplants and previously documented in liver transplant rejection.^{54,63,81} The R4_{late} group was distinct, with increased histologic fibrosis and elevated IGTs, MCATs, and BATs, similar to changes in long-term pediatric liver transplants with interface inflammation.⁸¹ Comparison between molecular findings and histology showed significant associations but extensive discrepancies. We conclude that RAT expression permits MMDx to detect TCMR, injury, and a late inflamed fibrosis state in small pieces of liver transplant biopsy cores.

The R1_{normal} score identified the biopsies with the absence of inflammation, injury, and fibrosis features and became the dominant phenotype with late TxBx. The predominance of high R1_{normal} scores at late time points and high R2_{TCMR} and R3_{injury} scores at earlier times underscores the unique time course of liver transplants compared with other transplanted organs, recovering from early injury and rejection to achieve long-term stability.

R2_{TCMR} was associated with typical TCMR transcripts and were relatively early posttransplant (median days posttransplant = 214), consistent with literature showing that the highest risk of TCMR was within the first month posttransplant with an incidence of 20%-40%.⁸² We propose to use the R2 and PC1 scores to assess the probability of rejection in a liver biopsy. The TCMR phenotype disappeared over time, perhaps reflecting T cell exhaustion as suggested for other transplants.^{43,83}

TABLE 4 Top 10 transcripts correlated with the RAT4A R1_{normal}, R2_{TCMR}, R3_{injury} and R4_{late} scores

R1 _{normal}		R2 _{TCMR}		R3 _{injury}		R4 _{late}	
Gene symbol	Correlation with R1 _{normal}	PBT annotations	Gene symbol	Correlation with R2 _{TCMR}	PBT annotations	Gene symbol	Correlation with R4 _{late}
TRIP12	-0.79	–	TAP1	0.90	GRIT, Rej-RAT, TCMR-RAT	JAM3	0.76
MIR21	-0.79	–	PSMB9	0.89	GRIT, Rej-RAT, TCMR-RAT	ELK3	0.75
IFNGR1	-0.79	–	STAT1	0.87	GRIT, IRRAT, TCMR-RAT	GYPC	0.74
FCGR1A	-0.78	GRIT, IRRAT, RAT, TCMR-RAT	PSMB8	0.87	GRIT, Rej-RAT	RAB34	0.74
ACTR3	-0.78	cIRIT, IRRAT, LivGST_UP	GBP5	0.87	GRIT, Rej-RAT	VIM	0.74
ACOT9	-0.78	LivGST_UP	PSMB10	0.85	GRIT, Rej-RAT, TCMR-RAT	DPYSL3	0.74
TMEM165	-0.78	IRRAT	GBP1	0.85	GRIT, Rej-RAT	SPARC	0.73
CAP1	-0.78	LivGST_UP	CXCL11	0.85	GRIT, Rej-RAT	LUM	0.73
DNM1L	-0.78	–	CXCL9	0.84	GRIT, Rej-RAT	ADGRA2	0.73
TMEM50A	-0.78	–	CTSS	0.84	GRIT, IRRAT, Rej-RAT	LTBP2	0.73

Note: Top transcripts were selected based on highest negative value of the Spearman correlation coefficient in R1, and highest positive value in R2–R4. Abbreviations: cIRIT, cardiac injury and repair-induced transcripts; GRIT, gamma-interferon and rejection-associated transcripts; IRRAT, injury and rejection-induced transcripts; LivGST_UP, liver transcripts (set 1) (increased during mouse liver rejection in gamma interferon receptor deficient [GRKO] liver transplants); PBT, pathogenesis-based transcripts; RAT, rejection-associated transcripts; Rej, Rejection; TCMR, T cell-mediated rejection.

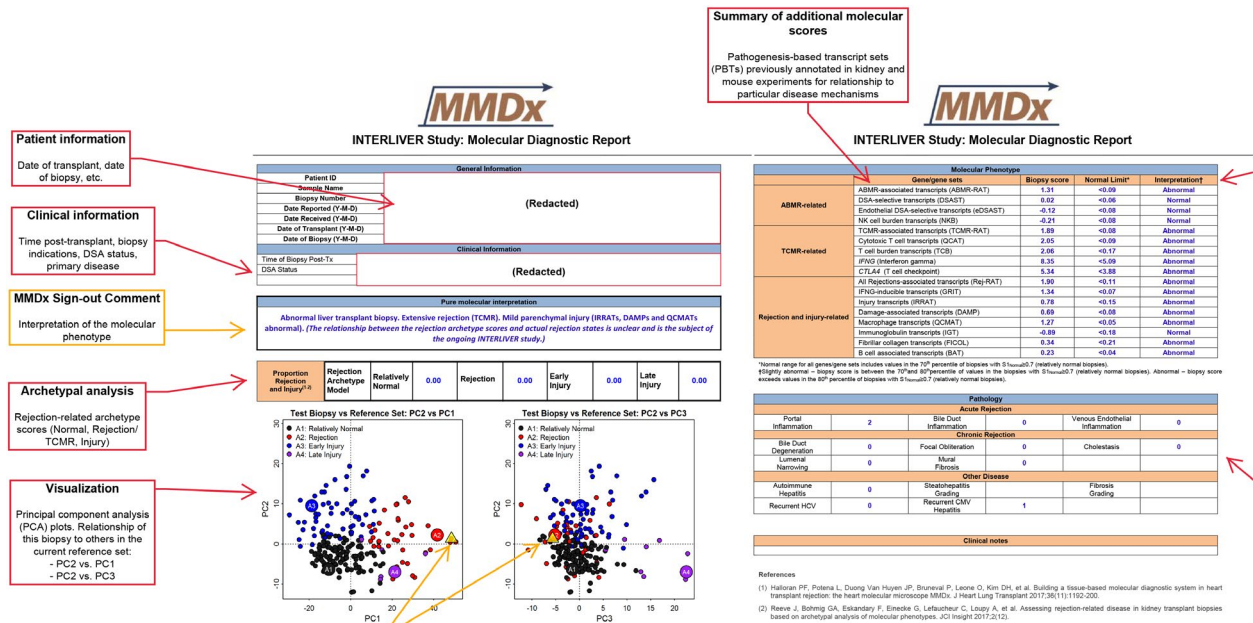


FIGURE 4 Example of the Molecular Microscope® Diagnostic System report on a new liver biopsy sample. The report is based on the reference set of 235 previously characterized liver biopsy samples. Left: page 1 of the report (molecular interpretation of the biopsy results, AA, PCA); right: page 2 of the report (additional molecular PBTs). The report is signed out by a single observer, providing the text-based interpretation (page 1). Interpretation of the biopsy (page 1) was based on the location of the biopsy in principal component 1, 2 and 3 (the figures on the report, page 1), the archetype assignment and scores (page 1), and the PBT scores (abnormal vs normal) on page 2

The $R_{3_{\text{injury}}}$ biopsies were associated with injury-related PBTs, had the earliest median TxTx, and strongly expressed hypoxia-inducible factor (HIF) EGLN, of interest given the role of HIFs in liver donation-implantation injury.⁸⁴ In contrast, $R_{4_{\text{late}}}$ biopsies were strongly associated with IGTs and BATs and MCATs, reflecting mild inflammatory infiltrate common in tissues undergoing atrophy-fibrosis. As previously mentioned, the $R_{4_{\text{late}}}$ group resembled biopsies with interface inflammation,⁸¹ with high expression of IGTs, MCATs, and BATs as well as a low level of TCMR-like inflammation. Liver fibrosis has been associated with B cell activity in other studies.^{85,86} The question remains whether this is a smoldering cognate alloimmune response (TCMR) or a late response-to-wounding. This group was small but minor increases in R_4 score in $R_1/R_2/R_3$ biopsies were common. Full exploration of late fibrosis-inflammation characteristics in liver transplants will require further analyses incorporating a wider range of transcripts than simply the RATs.

Although the incidence of ABMR in liver transplants remains unresolved, the present study does not support the concept of a common liver transplant ABMR state analogous to that in heart and kidney transplants. Liver ABMR phenotypes have been contentious since the beginnings of liver transplantation. We do not claim to be able to identify ABMR in troubled liver transplants at this time, because the diagnosis was not made in these centers and because our unsupervised search in Figure 1 did not reveal a separation of ABMR-RAT transcripts from TCMR-RAT transcripts in PC2. Most of our contributing centers do not believe that an ABMR phenotype is identifiable in their population, at least not with any frequency.

As approved by the institutional review boards, this study could not dictate that DSA be performed routinely because the study was precluded from changing the SOC in the participating centers. Previously annotated endothelial transcripts associated with ABMR in kidney transplant biopsies were elevated in $R_{4_{\text{late}}}$ biopsies, but this probably reflects angiogenesis in grafts undergoing fibrogenesis and actively forming atrophy-fibrosis. DSA testing is not SOC in liver transplantation and more DSA data would be very welcome to help solve the ABMR issue. But DSA can be misleading: the presence of DSA in a troubled liver transplant may simply be a marker of an alloresponse.⁸⁷ DSA appears with increasing frequency as time posttransplant increased in all organ transplant populations and is often not responsible for a phenotype: troubled transplants with late TCMR will be associated with DSA even if the phenotype is T cell driven. Thus late TCMR occurring during nonadherence or in immunosuppressive withdrawal studies ("chronic rejection") may be DSA positive^{88,89} and does not necessarily indicate a distinctive ABMR state. Moreover, early ABMR reported in ABO-incompatible and highly sensitized patients is now very uncommon and no cases were suspected in this cohort, and our studies can make no statement about phenotypes that do not exist in the study cohort. The molecular phenotype of liver ABMR remains an unresolved topic of strong interest, given the interest in immunosuppressive withdrawal and tolerance,^{21-22,90} and failure to find it by the tests applied in this study may simply be due to underrepresentation in the present biopsy cohort. Liver ABMR phenotypes have been contentious since the beginnings of liver transplantation. The next step will be to develop classifiers based on cases our collaborators

TABLE 5 Correlations between RAT4A archetype scores, PC scores, and high scores for histologic features (>0) in liver biopsies (N = 235)

Histology features	PC1	PC2	PC3	R1 _{normal} score	R2 _{TcMR} score	R3 _{injury} score	R4 _{late} score	NA (# of missing values)
Acute rejection: portal inflammation	0.27, P = 4E-05	0.01, P = 9E-01	-0.07, P = 3E-01	-0.09, P = 2E-01	0.29, P = 9E-06	-0.14, P = 3E-02	0.03, P = 6E-01	13
	0.21, P = 2E-03	-0.05, P = 4E-01	-0.06, P = 4E-01	-0.04, P = 6E-01	0.20, P = 4E-03	-0.14, P = 3E-02	0.05, P = 5E-01	15
Acute rejection: bile duct inflammation								
Acute rejection: venous inflammation	0.19, P = 4E-03	-0.11, P = 1E-01	0.00, P = 1E+00	-0.00, P = 1E+00	0.16, P = 2E-02	-0.19, P = 5E-03	0.11, P = 9E-02	14
Chronic rejection: bile duct degeneration	0.09, P = 2E-01	0.00, P = 1E+00	0.07, P = 3E-01	-0.08, P = 2E-01	0.03, P = 6E-01	0.01, P = 9E-01	0.12, P = 8E-02	20
Chronic rejection: focal obliteration	0.15, P = 3E-02	0.01, P = 9E-01	0.08, P = 3E-01	-0.14, P = 4E-02	0.09, P = 2E-01	-0.03, P = 7E-01	0.11, P = 9E-02	18
Chronic rejection: cholestasis	0.05, P = 5E-01	0.18, P = 7E-03	0.17, P = 1E-02	-0.26, P = 8E-05	0.01, P = 9E-01	0.16, P = 2E-02	0.17, P = 1E-02	18
Chronic rejection: mural fibrosis	0.09, P = 2E-01	0.07, P = 3E-01	0.07, P = 3E-01	-0.16, P = 2E-02	-0.02, P = 8E-01	0.10, P = 1E-01	0.10, P = 1E-01	18
Other disease: autoimmune hepatitis	0.14, P = 4E-02	0.07, P = 3E-01	0.03, P = 6E-01	-0.15, P = 3E-02	0.12, P = 8E-02	0.05, P = 5E-01	0.11, P = 1E-01	20
Other disease: steatohepatitis	0.01, P = 9E-01	0.12, P = 1E-01	-0.03, P = 7E-01	-0.04, P = 6E-01	0.05, P = 5E-01	0.11, P = 1E-01	-0.02, P = 8E-01	54
Other disease: fibrosis	-0.05, P = 5E-01	-0.33, P = 5E-06	0.31, P = 3E-05	0.27, P = 3E-04	-0.17, P = 3E-02	-0.18, P = 1E-02	0.28, P = 1E-04	56
Other disease: recurrent HCV	0.14, P = 5E-02	0.25, P = 2E-04	-0.08, P = 2E-01	-0.22, P = 1E-03	0.20, P = 3E-03	0.18, P = 1E-02	-0.05, P = 5E-01	21
Other disease: suspected CMV hepatitis	0.22, P = 9E-04	0.02, P = 8E-01	-0.23, P = 8E-04	-0.14, P = 4E-02	0.24, P = 5E-04	-0.13, P = 6E-02	-0.12, P = 8E-02	18

Note: Clinical data were binarized for this analysis. Sum score of portal, bile duct, and venous inflammation grades >0 was considered positive, 0 if negative. Spearman correlation coefficients are given alongside P values approximated from the value of the coefficient. Shaded cells are those considered significant based on the absolute value of the Spearman correlation coefficient >0.2.

TABLE 6 Laboratory test data for biopsies in INTERLIVER by RAT4A archetype group

Values in biopsies belonging to designated archetype group	Tests					
	Albumin g/dL mean (median, range) (N = 200)	Bilirubin mg/dL mean (median, range) (N = 226)	AST IU/L mean (median, range) (N = 226)	ALT IU/L mean (median, range) (N = 226)	ALP IU/L mean (median, range) (N = 225)	Time posttransplant in days mean (median, range)
RAT archetype groups						
R1 _{normal} (N = 129)	4.3 (4.3, 3.2-5.4) N = 102	1.2 (0.7, 0.1-36.0) N = 123	39.0 (27.0, 11-165) N = 123	51.8 (32.0, 8-289) N = 123	126.4 (95.0, 29-632) N = 123	2534 (2152, 58-9169) N = 129
R2 _{TCMR} (N = 37)	3.6 (3.6, 2.2-4.7) N = 33	2.8 (1.2, 0.2-18.9) N = 36	176.2 (95.0, 21-848) N = 36	214.9 (146.5, 27-815) N = 36	319.9 (189.0, 67-1467) N = 35	777 (214, 7-4918) N = 37
R3 _{injury} (N = 61)	3.4 (3.5, 1.9-4.7) N = 58	3.4 (1.9, 0.2-20.0) N = 59	274.5 (70.0, 17-5779) N = 58	205.2 (113.0, 9-1781) N = 59	273.7 (190.0, 54-1863) N = 59	814 (99, 0-5622) N = 61
R4 _{late} (N = 8)	3.1 (2.9, 1.7-4.4) N = 7	5.2 (1.5, 0.2-26.6) N = 8	110.5 (96.5, 19-292) N = 8	61.25 (59.0, 20-127) N = 8	353.8 (261.0, 166-890) N = 8	4807 (3117, 350-11676) N = 8

Note: ALP measurements showed significant differences between R2 biopsies and normal (R1 biopsies). No statistically significant differences were seen between R2 and other groups for bilirubin, or AST. Highlighted cells are the highest value in the column.

consider definite ABMR, but this will require a separate study with larger enrollment.

The relationship between histologic rejection (>0, >1, or >2 classifications) and MMDx diagnoses of TCMR was consistent with that seen in kidney and heart biopsies, taking into account the kappa values for histology in each organ. The choice of threshold for histologic rejection (0, 1, or 2) did not significantly alter the balanced accuracy, suggesting that the severity of recorded lesions did not significantly affect overall association with the MMDx rejection diagnoses. SOC histology assessment in these centers does not typically include a summary sign-out. Because these analyses focused purely on the relationships between MMDx and unmodified SOC, we used only the available information and interpreted this as was necessary for analyses requiring binary classes. Future analyses may include a classifier based on a more definitive style of diagnostic classification if this information can be obtained.

The limitations of this first-generation MMDx study include its relatively small number of samples and the lack of information regarding DSA information and infectious complications. Follow-up times after biopsy remain relatively short, with too few failures or retransplants to analyze survival or clinical outcomes at present. The ongoing INTERLIVER study should resolve these issues for future analyses. Supervised analysis was limited by SOC text-based reports. Although sampling error is a concern in all biopsy-based testing, prior analyses by the group have shown that the effect of sampling is low on MMDx assessments.³⁰ Biological replication in liver biopsies was also high, confirming that biopsies of the size and yield used in this study are appropriate for reliable MMDx assessment.

As in other MMDx studies, central pathology readings were not included, because the study design focused on comparisons to the SOC. Moreover, prior experience with central pathology readings did not reveal advantages in this approach because multiple central reviewers did not agree with one another.^{91,92} However, we acknowledge that this point of view is not universal, and central pathology review may be advisable in some future studies.

We conclude that liver transplant biopsies can be successfully assessed using a genome-wide discovery approach, and this assessment correlates with the current SOC histology classification of biopsies. Although distinct TCMR, injury, and late fibrosis states emerged, no distinct ABMR state was identified using approaches that revealed ABMR syndromes in kidney and heart transplants. There were considerable discrepancies with SOC histology as expected given the limited reproducibility (kappa values) in histology diagnoses: molecular tests cannot agree with histology more than histology agrees with itself. However, the ongoing INTERLIVER study and emerging technology of MMDx-Liver provide an opportunity to study the discrepancies to calibrate MMDx readings and recalibrate histology readings.

Although this emerging technology shows promise for diagnostics in liver transplantation, the INTERLIVER study is ongoing and a larger cohort is being collected to establish the clinical impact.

TABLE 7 Characterizing the relationship between histologic and molecular diagnoses in the liver biopsy population (N = 235)

Crosstab of individual histology features of acute rejection and overall histologic rejection vs molecular rejection sign-out comments							
				MMDx-Liver sign-outs (% of column)		Row totals	
				No rejection	TCMR		
Overall histologic acute rejection >0 ^a							
No rejection				51 (33%)	7 (11%)	58	
Rejection				104 (67%)	58 (89%)	162	
Column totals				155	65	220	
Overall histologic acute rejection >1 ^b							
No rejection				102 (66%)	23 (35%)	125	
Rejection				53 (34%)	42 (65%)	95	
Column totals				155	65	220	
Overall histologic acute rejection >2 ^c							
No rejection				124 (80%)	39 (60%)	163	
Rejection				31 (20%)	26 (40%)	57	
Column totals				155	65	220	
Confusion matrix statistics for MMDx diagnoses predicting the histologic diagnosis in liver transplant acute rejection							
Reference standard	Diagnostic test	Sensitivity	Specificity	Positive predictive value	Negative predictive value	Accuracy	Balanced accuracy
Histologic rejection lesion score >0 ^a	MMDx diagnosis ^d	0.36	0.89	0.89	0.33	0.50	0.62
Histologic rejection lesion score >1 ^b	MMDx diagnosis ^d	0.44	0.82	0.65	0.66	0.65	0.63
Histologic rejection lesion score >2 ^c	MMDx diagnosis ^d	0.46	0.76	0.40	0.80	0.68	0.60

^aBased on our algorithm interpreting the acute rejection scores/features, where the presence of any score >0 in portal, bile duct, or venous inflammation classified the biopsy as acute rejection. Samples with missing information were excluded from this analysis (N = 15), except where those samples were missing a single score and already clearly met the threshold for histologic rejection sum >0 (N = 2).

^bBased on our algorithm interpreting the acute rejection scores/features, where the presence of any score >1 in portal, bile duct, or venous inflammation classified the biopsy as acute rejection. Samples with missing information were excluded from this analysis (N = 15), except where those samples were missing a single score and already clearly met the threshold for histologic rejection sum >1 (N = 2).

^cBased on our algorithm interpreting the acute rejection scores/features, where the presence of any score >2 in portal, bile duct, or venous inflammation classified the biopsy as acute rejection. Samples with missing information were excluded from this analysis (N = 15), except where those samples were missing a single score and already clearly met the threshold for histologic rejection sum >1 (N = 2).

^dBased on the diagnosis of acute rejection (TCMR) or no rejection by an expert signing out the official MMDx report. Diagnoses were based on position of the biopsy in the report figure, archetypal data, and PBT information provided on page 2.

Future studies now focus on understanding more phenotypes such as the molecular identification of steatohepatitis, the resolution of the question of liver ABMR, and outcome analysis once follow-up data become available. The future studies also aim to engage the expert pathologists to understand the clinical states using both histology criteria and the molecular findings and derive an integrated classification.

ACKNOWLEDGMENTS

This research has been supported by funding and/or resources from Genome Canada, Canada Foundation for Innovation, the University of Alberta Hospital Foundation, the Alberta Ministry of Advanced Education and Technology, the Mendez National Institute of Transplantation Foundation, Industrial Research Assistance

Program, and the Roche Organ Transplant Research Foundation. Partial support was also provided by funding from a licensing agreement with the One Lambda division of Thermo Fisher. Dr Halloran held a Canada Research Chair in Transplant Immunology until 2008 and currently holds the Muttart Chair in Clinical Immunology.

DISCLOSURE

The authors of this manuscript have conflicts of interest to disclose as described by the *American Journal of Transplantation*. P. F. Halloran holds shares in Transcriptome Sciences Inc, a University of Alberta research company with an interest in molecular diagnostics, has given lectures for Thermo Fisher and is a consultant for CSL Behring. The other authors have no conflicts of interest to disclose.

DATA AVAILABILITY STATEMENT

The .CEL files are available at Gene Expression Omnibus (GEO) (GSE145780) as stated in Section 2.2 of the article.

ORCID

Goran Klintmalm  <https://orcid.org/0000-0003-0916-6042>

Trevor Reichman  <https://orcid.org/0000-0002-2303-1606>

Alberto Sanchez-Fueyo  <https://orcid.org/0000-0002-8316-3504>

Philip F. Halloran  <https://orcid.org/0000-0003-1371-1947>

REFERENCES

- McCaughan GW, Gorrell MD, Alex Bishop G, et al. Molecular pathogenesis of liver disease: an approach to hepatic inflammation, cirrhosis and liver transplant tolerance. *Immunol Rev*. 2000;174:172-191.
- Neuberger J. An update on liver transplantation: a critical review. *J Autoimmun*. 2016;66:51-59.
- Zarrinpar A, Busuttil RW. Liver transplantation: past, present and future. *Nat Rev Gastroenterol Hepatol*. 2013;10(7):434-440.
- Wadström J, Ericzon B-G, Halloran PF, et al. Advancing transplantation: new questions, new possibilities in kidney and liver transplantation. *Transplantation*. 2017;101(Suppl 2S):S1-S41.
- Demetris AJ, Bellamy C, Hübscher SG, et al. 2016 Comprehensive update of the banff working group on liver allograft pathology: introduction of antibody-mediated rejection. *Am J Transplant*. 2016;16(10):2816-2835.
- Fisher LR, Henley KS, Lucey MR. Acute cellular rejection after liver transplantation: variability, morbidity, and mortality. *Liver Transpl Surg*. 1995;1(1):10-15.
- Regev A, Molina E, Moura R, et al. Reliability of histopathologic assessment for the differentiation of recurrent hepatitis C from acute rejection after liver transplantation. *Liver Transpl*. 2004;10(10):1233-1239.
- Younossi ZM, Boparai N, Gramlich T, Goldblum J, George P, Mayes J. Agreement in pathologic interpretation of liver biopsy specimens in posttransplant hepatitis C infection. *Arch Pathol Lab Med*. 1999;123(2):143-145.
- Pournik O, Alavian SM, Ghalichi L, et al. Inter-observer and intra-observer agreement in pathological evaluation of non-alcoholic fatty liver disease suspected liver biopsies. *Hepat Mon*. 2014;14(1):e15167.
- Wiesner RH. Is hepatic histology the true gold standard in diagnosing acute hepatic allograft rejection? *Liver Transpl Surg*. 1996;2(2):165-167.
- Horvath B, Allende D, Xie H, et al. Interobserver variability in scoring liver biopsies with a diagnosis of alcoholic hepatitis. *Alcohol Clin Exp Res*. 2017;41(9):1568-1573.
- Netto GJ, Watkins DL, Williams JW, et al. Interobserver agreement in hepatitis C grading and staging and in the Banff grading schema for acute cellular rejection - the "Hepatitis C 3" multi-institutional trial experience. *Arch Pathol Lab Med*. 2006;130(8):1157-1162.
- Lee M. Antibody-mediated rejection after liver transplant. *Gastroenterol Clin North Am*. 2017;46(2):297-309.
- Taner T, Stegall MD, Heimbach JK. Antibody-mediated rejection in liver transplantation: current controversies and future directions. *Liver Transpl*. 2014;20(5):514-527.
- Dao M, Habès D, Taupin J-L, et al. Morphological characterization of chronic antibody-mediated rejection in ABO-identical or ABO-compatible pediatric liver graft recipients. *Liver Transpl*. 2018;24(7):897-907.
- Clavien PA, Muller X, de Oliveira ML, Dutkowski P, Sanchez-Fueyo A. Can immunosuppression be stopped after liver transplantation? *Lancet Gastroenterol Hepatol*. 2017;2(7):531-537.
- Ascha MS, Ascha ML, Hanouneh IA. Management of immunosuppressant agents following liver transplantation: less is more. *World J Hepatol*. 2016;8(3):148-161.
- Cheng EY, Terasaki PI. Tolerogenic mechanisms in liver transplantation. *SOJ Immunology*. 2015;3(4):1-13.
- Moini M, Schilsky ML, Tichy EM. Review on immunosuppression in liver transplantation. *World J Hepatol*. 2015;7(10):1355-1368.
- Lerut J, Sanchez-Fueyo A. An appraisal of tolerance in liver transplantation. *Am J Transplant*. 2006;6(8):1774-1780.
- Savage TM, Shonts BA, Lau S, et al. Deletion of donor-reactive T cell clones following human liver transplantation. *Am J Transplant*. 2020;20(2):538-545.
- Levitsky J, Feng S. Tolerance in clinical liver transplantation. *Hum Immunol*. 2018;79(5):283-287.
- Thomson AW, Knolle PA. Antigen-presenting cell function in the tolerogenic liver environment. *Nat Rev Immunol*. 2010;10(11):753-766.
- Vionnet J, Sanchez-Fueyo A. Biomarkers of immune tolerance in liver transplantation. *Hum Immunol*. 2018;79(5):388-394.
- Mastoridis S, Martinez-Llordella M, Sanchez-Fueyo A. Emergent transcriptomic technologies and their role in the discovery of biomarkers of liver transplant tolerance. *Front Immunol*. 2015;6:304.
- Mofrad P, Contos MJ, Haque M, et al. Clinical and histologic spectrum of nonalcoholic fatty liver disease associated with normal ALT values. *Hepatology*. 2003;37(6):1286-1292.
- Sorrentino P, Tarantino G, Conca P, et al. Silent non-alcoholic fatty liver disease-a clinical-histological study. *J Hepatol*. 2004;41(5):751-757.
- Topol E. *Deep Medicine: How Artificial Intelligence Can Make Healthcare Human Again* (1st ed.). New York, NY: Basic Books; 2019:341.
- Reeve J, Böhmig GA, Eskandary F, et al. Generating automated kidney transplant biopsy reports combining molecular measurements with ensembles of machine learning classifiers. *Am J Transplant*. 2019;19(10):2719-2731.
- Madill-Thomsen KS, Wiggins RC, Eskandary F, Böhmig GA, Halloran PF. The effect of cortex/medulla proportions on molecular diagnoses in kidney transplant biopsies: rejection and injury can be assessed in medulla. *Am J Transplant*. 2017;17(8):2117-2128.
- Halloran PF, Reeve J, Akalin E, et al. Real time central assessment of kidney transplant indication biopsies by microarrays: the INTERCOMEX study. *Am J Transplant*. 2017;17(11):2851-2862.
- Madill-Thomsen K, Perkowska-Ptasińska A, Böhmig GA, et al. Discrepancy analysis comparing molecular and histology diagnoses in kidney transplant biopsies. *Am J Transplant*. 2020. <https://doi.org/10.1111/ajt.15752>
- Reeve J, Kim DH, Crespo-Leiro MG, et al. Molecular diagnosis of rejection phenotypes in 889 heart transplant biopsies: the INTERHEART study. *J Heart Lung Transplant*. 2018;37(4):S27.
- Halloran PF, Reeve J, Aliabadi AZ, et al. Exploring the cardiac response to injury in heart transplant biopsies. *JCI Insight*. 2018;3(20):e123674.
- Parkes M, Halloran K, Famulski K, Halloran P, Grp IS. Molecular phenotypes of injury and rejection in lung transplant transbronchial biopsies. *Am J Transplant*. 2018;18(S4):274-275.
- Halloran KM, Parkes MD, Chang J, et al. Molecular assessment of rejection and injury in lung transplant biopsies. *J Heart Lung Transplant*. 2019;38(5):504-513.
- Halloran K, Parkes MD, Timofte IL, et al. Molecular phenotyping of rejection-related changes in mucosal biopsies from lung transplants. *Am J Transplant*. 2019. <https://doi.org/10.1111/ajt.15685>
- Einecke G, Reeve J, Sis B, et al. A molecular classifier for predicting future graft loss in late kidney transplant biopsies. *J Clin Invest*. 2010;120(6):1862-1872.

39. Halloran PF, Pereira AB, Chang J, et al. Microarray diagnosis of antibody-mediated rejection in kidney transplant biopsies: an international prospective study (INTERCOM). *Am J Transplant.* 2013;13(11):2865-2874.
40. Famulski KS, Reeve J, de Freitas DG, Kreepala C, Chang J, Halloran PF. Kidney transplants with progressing chronic diseases express high levels of acute kidney injury transcripts. *Am J Transplant.* 2013;13(3):634-644.
41. Halloran PF, Matas A, Kasiske BL, Madill-Thomsen KS, Mackova M, Famulski KS. Molecular phenotype of kidney transplant indication biopsies with inflammation in scarred areas. *Am J Transplant.* 2019;19(5):1356-1370.
42. Einecke G, Reeve J, Halloran P. Predictors of graft survival at the time of a kidney transplant indication biopsy. *Am J Transplant.* 2018;18(5):370.
43. Halloran PF, Chang J, Famulski K, et al. Disappearance of T cell-mediated rejection despite continued antibody-mediated rejection in late kidney transplant recipients. *J Am Soc Nephrol.* 2015;26(7):1711-1720.
44. Halloran PF, Famulski KS, Reeve J. Molecular assessment of disease states in kidney transplant biopsy samples. *Nat Rev Nephrol.* 2016;12(9):534-548.
45. Venner JM, Hidalgo LG, Famulski KS, Chang J, Halloran PF. The molecular landscape of antibody-mediated kidney transplant rejection: evidence for NK involvement through CD16a Fc receptors. *Am J Transplant.* 2015;15(5):1336-1348.
46. Halloran P, Kim D, Loupy A, et al. Development and validation of a molecular microscope diagnostic system (MMDx) for Heart Transplant Biopsies. *American Journal of Transplantation.* 2016;16(4S):332.
47. Halloran PF, Reeve J, Group IS. Validating the INTERHEART classifiers for molecular diagnosis of rejection in 437 new endomyocardial biopsies. *J Heart Lung Transplant.* 2018;37(5):S303-S304.
48. Parkes M, Reeve J, Kim D, et al. Molecular assessment of heart transplant biopsies: emergence of the injury dimension. *Transplantation.* 2018;102:S62-S63.
49. Halloran K, Parkes MD, Chang J, et al. Molecular detection of rejection-like changes in proximal bronchial mucosal lung transplant biopsies: initial findings of the INTERLUNG study. *J Heart Lung Transplant.* 2018;37(4):S80-S81.
50. Okubo K, Wada H, Tanaka A, et al. Identification of novel and non-invasive biomarkers of acute cellular rejection after liver transplantation by protein microarray. *Transplant Direct.* 2016;2:e118.
51. Inkinen K, Lahesmaa R, Brandt A, et al. DNA microarray-based gene expression profiles of cytomegalovirus infection and acute rejection in liver transplants. *Transplant Proc.* 2005;37(2):1227-1229.
52. Muffak-Granero K, Bueno P, Olmedo C, et al. Study of gene expression profile in liver transplant recipients with hepatitis C virus. *Transplant Proc.* 2008;40(9):2971-2974.
53. Šeda O, Cahová M, Míková I, et al. Hepatic gene expression profiles differentiate steatotic and non-steatotic grafts in liver transplant recipients. *Front Endocrinol (Lausanne).* 2019;10:270.
54. Londoño M-C, Souza LN, Lozano J-J, et al. Molecular profiling of subclinical inflammatory lesions in long-term surviving adult liver transplant recipients. *J Hepatol.* 2018;69(3):626-634.
55. Lozano JJ, Pallier A, Martinez-Llordella M, et al. Comparison of transcriptional and blood cell-phenotypic markers between operationally tolerant liver and kidney recipients. *Am J Transplant.* 2011;11(9):1916-1926.
56. Spivey TL, Uccellini L, Ascierto M, et al. Gene expression profiling in acute allograft rejection: challenging the immunologic constant of rejection hypothesis. *J Transl Med.* 2011;9:174.
57. Halloran PF, Venner JM, Madill-Thomsen KS, et al. Review: the transcripts associated with organ allograft rejection. *Am J Transplant.* 2018;18(4):785-795.
58. Halloran PF, Potena L, Van Huyen J-P, et al. Building a tissue-based molecular diagnostic system in heart transplant rejection: the heart molecular microscope diagnostic (MMDx) system. *J Heart Lung Transplant.* 2017;36(11):1192-1200.
59. Loupy A, Duong Van Huyen JP, Hidalgo L, et al. Gene expression profiling for the identification and classification of antibody-mediated heart rejection. *Circulation.* 2017;135(10):917-935.
60. Halloran PF, Venner JM, Famulski KS. Comprehensive analysis of transcript changes associated with allograft rejection: combining universal and selective features. *Am J Transplant.* 2017;17(7):1754-1769.
61. ATAGC. Gene Lists 2019. <https://www.ualberta.ca/medicine/institutes-centres-groups/atagc/research/gene-lists>. Accessed January 10, 2020.
62. Martínez-Llordella M, Puig-Pey I, Orlando G, et al. Multiparameter immune profiling of operational tolerance in liver transplantation. *Am J Transplant.* 2007;7(2):309-319.
63. Bonaccorsi-Riani E, Pennycuik A, Londoño M-C, et al. Molecular characterization of acute cellular rejection occurring during intentional immunosuppression withdrawal in liver transplantation. *Am J Transplant.* 2016;16(2):484-496.
64. Einecke G, Reeve J, Mengel M, et al. Expression of B cell and immunoglobulin transcripts is a feature of inflammation in late allografts. *Am J Transplant.* 2008;8(7):1434-1443.
65. Mengel M, Sis B, Kim D, et al. The molecular phenotype of heart transplant biopsies: relationship to histopathological and clinical variables. *Am J Transplant.* 2010;10(9):2105-2115.
66. Land WG, Agostinis P, Gasser S, Garg AD, Linkermann A. Transplantation and damage-associated molecular patterns (DAMPs). *Am J Transplant.* 2016;16(12):3338-3361.
67. Hidalgo LG, Sellares J, Sis B, Mengel M, Chang J, Halloran PF. Interpreting NK cell transcripts versus T cell transcripts in renal transplant biopsies. *Am J Transplant.* 2012;12(5):1180-1191.
68. Einecke G, Sis B, Reeve J, et al. Antibody-mediated microcirculation injury is the major cause of late kidney transplant failure. *Am J Transplant.* 2009;9(11):2520-2531.
69. Famulski KS, Einecke G, Reeve J, et al. Changes in the transcriptome in allograft rejection: IFN- γ induced transcripts in mouse kidney allografts. *Am J Transplant.* 2006;6(6):1342-1354.
70. Famulski KS, Broderick G, Einecke G, et al. Transcriptome analysis reveals heterogeneity in the injury response of kidney transplants. *Am J Transplant.* 2007;7(11):2483-2495.
71. Famulski KS, de Freitas DG, Kreepala C, et al. Molecular phenotypes of acute kidney injury in human kidney transplants. *J Am Soc Nephrol.* 2012;23(5):948-958.
72. Mengel M, Reeve J, Bunnag S, et al. Molecular correlates of scarring in kidney transplants: the emergence of mast cell transcripts. *Am J Transplant.* 2009;9(1):169-178.
73. Hidalgo LG, Einecke G, Allanach K, et al. The transcriptome of human cytotoxic T cells: measuring the burden of CTL-associated transcripts in human kidney transplants. *Am J Transplant.* 2008;8(3):637-646.
74. RCT. R: A Language and Environment for Statistical Computing. Vienna, Austria: R Foundation for Statistical Computing; 2019. <http://www.r-project.org/>. Accessed January 11, 2020.
75. Lê S, Josse J, Husson F. FactoMineR: an R package for multivariate analysis. *J Stat Soft.* 2008;25(1):18.
76. Reeve J, Böhmig GA, Eskandary F, et al. Assessing rejection-related disease in kidney transplant biopsies based on archetypal analysis of molecular phenotypes. *JCI Insight.* 2017;2(12):e94197.
77. Eugster MJA, Leisch F. From spider-man to hero - archetypal analysis in R. *J Stat Soft.* 2009;30(8):1-23.
78. Zeileis A, Grothendieck G. Zoo: S3 Infrastructure for regular and irregular time series. *J Stat Softw.* 2005;14:1-27.
79. Demetrius AJ, Batts KP, Dhillon AP, et al. Banff schema for grading liver allograft rejection: an international consensus document. *Hepatology.* 1997;25(3):658-663.

80. Robin X, Turck N, Hainard A, et al. pROC: an open-source package for R and S+ to analyze and compare ROC curves. *BMC Bioinformatics*. 2011;2011(12):77.
81. Feng S, Bucuvalas JC, Demetris AJ, et al. Evidence of chronic allograft injury in liver biopsies from long-term pediatric recipients of liver transplants. *Gastroenterology*. 2018;155(6):1838-1851.e7.
82. Dogan N, Husing-Kabar A, Schmidt HH, Cicinnati VR, Beckebaum S, Kabar I. Acute allograft rejection in liver transplant recipients: incidence, risk factors, treatment success, and impact on graft failure. *J Int Med Res*. 2018;46(9):3979-3990.
83. Venner JM, Famulski KS, Badr D, Hidalgo LG, Chang J, Halloran PF. Molecular landscape of T cell-mediated rejection in human kidney transplants: prominence of CTLA4 and PD ligands. *Am J Transplant*. 2014;14(11):2565-2576.
84. Dar WA, Sullivan E, Bynon JS, Eltzschig H, Ju C. Ischaemia reperfusion injury in liver transplantation: cellular and molecular mechanisms. *Liver International*. 2019;39:788-801.
85. Faggioli F, Palagano E, Di Tommaso L, et al. B lymphocytes limit senescence-driven fibrosis resolution and favor hepatocarcinogenesis in mouse liver injury. *Hepatology*. 2018;67(5):1970-1985.
86. Novobrantseva TI, Majeau GR, Amatucci A, et al. Attenuated liver fibrosis in the absence of B cells. *J Clin Invest*. 2005;115(11):3072-3082.
87. Jucaud V, Shaked A, DesMarais M, et al. Prevalence and impact of de novo donor-specific antibodies during a multicenter immunosuppression withdrawal trial in adult liver transplant recipients. *Hepatology*. 2019;69(3):1273-1286.
88. Kaneku H, O'Leary JG, Taniguchi M, Susskind BM, Terasaki PI, Klintmalm GB. Donor-specific human leukocyte antigen antibodies of the immunoglobulin G3 subclass are associated with chronic rejection and graft loss after liver transplantation. *Liver Transpl*. 2012;18(8):984-992.
89. O'Leary JG, Kaneku H, Susskind BM, et al. High mean fluorescence intensity donor-specific anti-HLA antibodies associated with chronic rejection postliver transplant. *Am J Transplant*. 2011;11(9):1868-1876.
90. Shaked A, DesMarais MR, Kopetskie H, et al. Outcomes of immunosuppression minimization and withdrawal early after liver transplantation. *Am J Transplant*. 2019;19(5):1397-1409.
91. Sellarés J, Reeve J, Loupy A, et al. Molecular diagnosis of antibody-mediated rejection in human kidney transplants. *Am J Transplant*. 2013;13(4):971-983.
92. Reeve J, Sellarés J, Mengel M, et al. Molecular diagnosis of T cell-mediated rejection in human kidney transplant biopsies. *Am J Transplant*. 2013;13(3):645-655.

SUPPORTING INFORMATION

Additional supporting information may be found online in the Supporting Information section.

How to cite this article: Madill-Thomsen K, Abouljoud M, Bhati C, et al. The molecular diagnosis of rejection in liver transplant biopsies: First results of the INTERLIVER study. *Am J Transplant*. 2020;20:2156–2172. <https://doi.org/10.1111/ajt.15828>